Current Results of the VERA K/Q-band Fringe Survey: Performance of the 8-Gbps Recording System and its Effectiveness

Takaaki Jike [1], Tomoaki Oyama [1], Takumi Nagayama [1], Aya Yamauchi [1]

Abstract VERA (VLBI Exploration of Radio Astrometry) started a K/Q-band continuum radio source fringe survey using an 8-Gbps recording system in January 2016. The main purposes of these experiments are the establishment of analysis procedures for highly sensitive VLBI (Very Long Baseline Interferometry) data, increasing the observable radio sources for VERA, and confirming the effect on the analysis results of the reduction of white noise error. The radio sources for observation are selected from the VLBA (Very Long Baseline Array) Calibrator List; some 5,196 radio sources, which are distributed in the range of −45 to 90 degrees of Celestial declination, are listed as observable candidates. The frequency fluctuation from atmospheric refraction and the instability of phase lock oscillators are corrected by smoothing, using a Moving-Average Filter, to inhibit a decrease of the correlation coefficient during the integration period. By May 2018, 3,252 sources in K-band and 2,941 sources in Q-band were observed. When the fringe detection was realized with signal-to-noise ratios of seven or more, the number of radio sources that met the fringe detection criterion was 2,608 in K-band and 1,725 in Q-band. From the delays of the 8-Gbps recorded VLBI data, the azimuthal anomaly of residual delays (including anisotropy of atmospheric excess pass delay) was confirmed.

Keywords VERA, 8-Gbps recording

1. Mizusawa VLBI Observatory, National Astronomical Observatory of Japan

1 Introduction

VERA is a Japanese VLBI project dedicated to phase-referencing astrometry. This project aims at determining annual parallaxes and proper motions of Galactic MASER (Microwave Amplification by Stimulated Emission of Radiation) emitting areas in the precision of a few tens of microarcseconds with reference to a nearby quasar on the celestial sphere.

A new sampling and recording system with a more than 8-Gbps rate capability is developed corresponding to a wide-band receiving system, and experimental fringe search observations have been carried out to confirm the fringe detection performance of this system. Serving as this experiment, VERA started a K/Q-band continuum radio source fringe survey using an 8-Gbps recording system in January 2016. The purposes of this experiment are reservation of the radio sources suitable for phase referencing by improving fringe detection sensitivity, establishment of the way for obtaining accurate fringes from wide band VLBI data, and fundamental research for the next plan for Mizusawa. Obtaining accurate fringes improves reliability also for geodetic and astrometric parameter estimation.

In this report, we present the results of the fringe survey performed by May 2018 and the fringe detection performance of the 8-Gbps recording system.

2 Formation of Data

The radio sources which become observable candidates are selected from the VLBA Calibrator List (http://www.vlba.nrao.edu/astro/calib). The distribution of observable radio sources on the celestial sphere

is shown in Figure 1, and the restrictions for selecting radio sources are shown in Table 1.

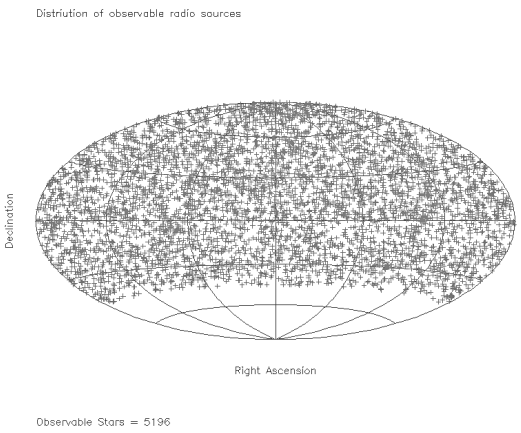

Fig. 1 Distribution of observable radio sources.

Table 1 Restrictions for selecting radio sources.

Version of main radio source list	160107
Total number of observable radio sources	5,196
Range of Right Ascension	0–24 hour
Range of Declination	−45 – 90 deg

A series of observations was carried out only in the VERA network. Specifications of the observation system which refer to fringe detection sensitivity are shown in Table 2. ADS3000+ and VSREC are adopted to the sampling—recording system. Observations were performed separately for each frequency band.

Table 2 Specifications of observation system.

Frequency Band Code	K	Q
Received Freq. band (GHz)	21.5–23.5	42.4–44.4
Typical SEFD (Jy)	439	848
Sampling and Filtering Mode	1,024 MHz, 2 bit, 4 stream	
Recording Bit Rate (Mbps)	8,196	

Correlation processing was done by the Mizusawa Software Correlator. Table 3 shows the settings of the correlation and fringe search. The basic package of fringe search software is regularly used in order to estimate delays from VERA internal geodetic VLBI data, and this software was given additional reconstruction for processing of this wide-band and highly sensitive VLBI data.

One of the main reconstructions is correcting the temporal fluctuations of fringe phases whose causes are frequency variations from atmospheric refraction and instability of the local reference frequency. The temporal fluctuations of fringe phases become large in proportion to frequency. Because the K- and Q-bands are high frequency, the temporal fluctuations of fringe phases are remarkable. The fluctuations degrade the coherency, and the fringe is dispersed along the rate direction; therefore, a suitable correlation amplitude corresponding to the integration time is not obtained. In order to remove the long-periodic component of fluctuations, smoothing by Low Pass Filter (LPF) was executed on the fluctuations. At the first onset, as one of the most fundamental digital LPFs, the Moving Average Filter was adopted for smoothing. The averaging period is nine seconds, which was estimated by Modified Allan Standard Deviation of phase temporal fluctuations. It was confirmed that the period from seven to eleven seconds is the zone where the character of fluctuations shifts from random walk to bias instability (Figure 2), almost in a fringe with a signal-to-noise ratio of 20.0 or more. Integration is again carried out, with modification of the phase along the smoothed line like the solid line shown in Figure 3.

Table 3 Correlation and fringe search settings.

Correlator Type	FX
The number of spectrum channels / stream	512
Frequency resolution / channel	1 MHz
Total correlated bandwidth	2048 MHz
Accumulation period	1 second
Effective integration bandwidth	1920 MHz
Integration period / 1 scan	128 seconds
Peak search method	2-D parabolic fitting

When the phase fluctuations of Figure 3 were modified, the signal-to-noise ratio of the fringes after fluctuation modification was 1.4 times larger in comparison to the one before modification. It is necessary to take care of the effect that coherency of noise increases. Before and after the smoothing process, the root mean square of the fringe phase differences was 0.67° at the central epoch in the integration time range; the large difference with respect to the estimation of the averaged fringe phase was not confirmed.

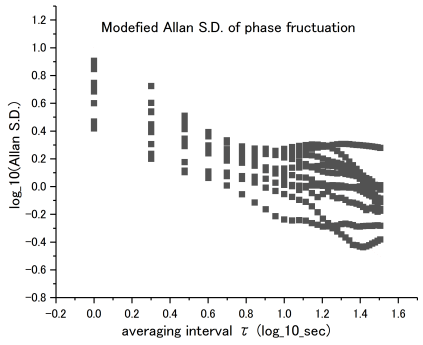

Fig. 2 Modified Allan Standard Deviations of fringe phase fluctuations.

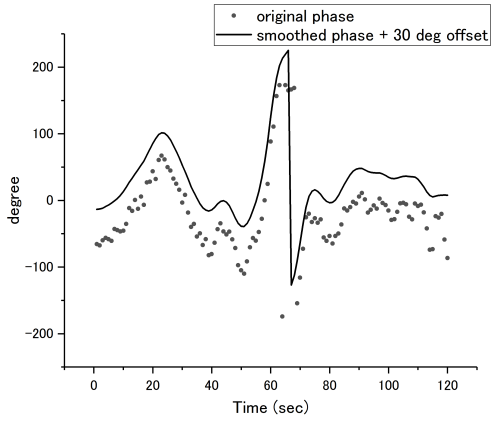

Fig. 3 Temporal fluctuation of fringe phases and smoothed line.

3 The Borderline of Fringe Recognition

The signal-to-noise ratio (S/N) is used for recognition of fringe detection as a standard. Usually, the analysis of VERA internal geodetic VLBI sets the criterion for recognition of fringe detection; the delay estimated from fringes with 7.0 or more S/N is used for parameter estimation. The Delay Deviation Score (*DDS*) is adopted in order to investigate the relationship between S/N and the accuracy of fringe tracking parameters. The delays used for estimation of the standard deviation in the calculation process of *DDS* are obtained from fringes with 7.0 or more S/N, applying the fringe recognition criterion of geodetic VLBI, and this is expressed by the following equations.

$$DDS = \{10(dly_{obs} - dly_{apr} - dly_{clk})/\sigma_{dly}\} + 50, \quad (1)$$

where dly_{obs} is the observed delay, dly_{apr} is the a-priori delay used for fringe tracking, dly_{clk} is the clock offset residual, σ_{dly} is the standard deviation of $dly_{SN7} - dly_{apr} - dly_{clk}$, and dly_{SN7} is dly_{obs} with 7.0 or more S/N. It is expected that *DDS* will congregate between 40 and 60 (the 1σ zone), when an accurate fringe tracking parameter is used for correlation processing. Therefore, when *DDS* of a fringe goes into the 1σ zone, it leads to the increase in probability that the S/N of this fringe is the signal-to-noise ratio of the fringe brought about from the signal of the radio source.

The relationship between S/N and *DDS* is shown in Figure 4. When S/N becomes 6.5 or more, *DDS*s congregate remarkably near the 1σ zone, and this tendency is the same with K- and Q-band. In order to show in detail the *DDS* distribution near where the concentration ratio changes, Figure 5 shows the ratios of fringes which fulfill specific restrictions. The ratio (R_{DDS}) is given as a percentage as follows,

$$R_{DDS} = \{n(S_{(DDS)} \cap S_{(S/N)})/n(S_{(S/N)})\} \times 100. \quad (2)$$

$S_{(DDS)}$ and $S_{(S/N)}$ in Equation 2 are the sets with restrictions expressed in the following,

$$\begin{aligned} S_{(DDS)} &= \{DDS \,|\, 40 \le DDS \le 50\}, \\ S_{(S/N)} &= \{S/N \,|\, SNR_1 \le S/N < SNR_2\}, \end{aligned} \quad (3)$$

where SNR_1 and SNR_2 are specific values of the signal-to-noise ratio showing the range of restrictions. As S/N increases from 5.5 to 7.0, the increasing rate of R_{DDS} becomes rapid; on the other hand, when S/N becomes larger than 7.0, the increasing rate of R_{DDS} declines. Therefore, when S/N is 7.0 or more, a fringe is mostly recognized to be detected, and when $6.0 \le S/N < 7.0$, recognition of fringe detection is marginal.

Even if S/N is high, several percent of radio sources remove *DDS* from the 1σ zone. A *DDS* which has a large gap from the 1σ zone arises from mistakes of fringe tracking. It is considered that the causes of fringe tracking mistakes are an instable reference frequency, inaccuracy of geometrical delay from the uncertainty of the radio source positions and ground-station positions, and error of the atmospheric excess pass delay model. Accumulation of fringe tracking errors decreases the correlation coefficient. It is required to re-

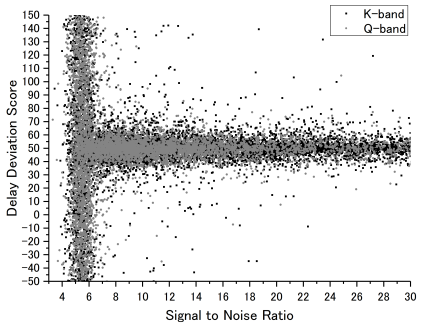

Fig. 4 Distribution of delay deviation score with respect to signal-to-noise ratio.

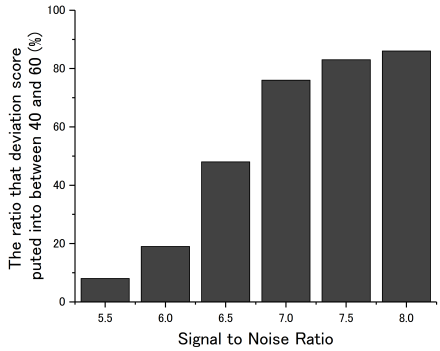

Fig. 5 The ratios of fringes with specific S/N score *DDS*s between 40 and 60.

duce these factors that obstruct accurate fringe tracking in order to obtain a more accurate fringe.

4 Results of Fringe Detection

In fringe survey observation, several fringe results are obtained from one radio source. The maximum signal-to-noise ratio in these fringe results is adopted as the decision of fringe detection. Table 4 shows the fringe detection results of the fringe search observations performed by May 2018. The fringes with 7.0 or more S/N were obtained from 80% of K- and 59% of Q-band radio sources.

For checking the minimum of the correlation flux density, Figure 6 shows the frequency distribution of less than 1.0 Jy correlation flux density. The minimum

Table 4 Fringe detection result.

	Number of sources	
Frequency Band Code	K	Q
Total number of observed	3,252	2,941
Fringe is detected	2,608	1,725
Fringe is marginal	378	730

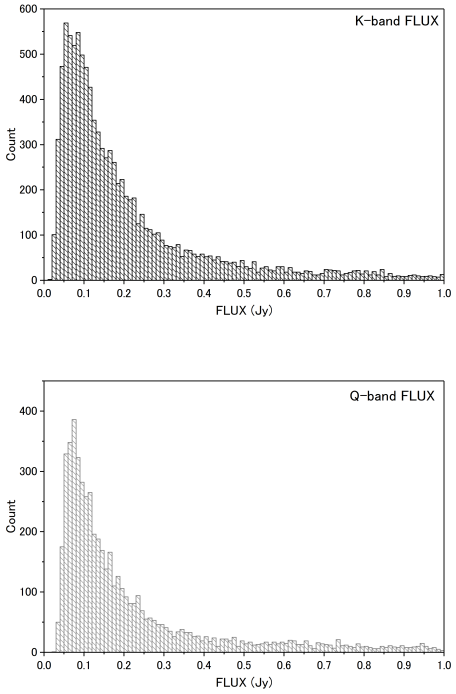

Fig. 6 Frequency distributions of less than 1.0 Jy correlation flux density.

flux density is 25 mJy in K- and 35 mJy in Q-band. The coherence loss factor used in order to estimate these correlation flux densities was 0.87. However, this factor is an ideal value for two-bit sampling and is not the actual value estimated corresponding to the efficiency of our wide band observation system, so these flux densities are provisional.

5 Azimuthal Anisotropy of Atmospheric Excess Pass Delay

A fringe tracking mistake removes the *DDS* from the 1σ zone, and it is surmised that one of the main causes

of fringe tracking mistakes is prediction errors of the atmospheric excess pass delay. Estimation of the atmospheric excess pass delay correction applied to the mapping function is effective for bringing the *DDS* close within the 1σ zone. However, although an observed delay with a few picoseconds of theoretical white noise error is obtained from 8-Gbps recording VLBI data, the root mean square of the post-fit-residual delay remained 14.0 picoseconds [1]. It is expected that the excess pass delays which do not suit the azimuthal-isotropic mapping function model are mixed in these residuals.

In order to confirm the azimuthal anisotropy of atmospheric excess path delay, we tried to get the distributions of $dly_{grad}(= dly_{rsd}/GMFW)$ in alignment with the azimuth. The used delays were obtained from VERA K-band internal geodetic VLBI using the OCTAD-OCTADISK2 8-Gbps sampling-recording system on November 27, 2017; theoretical white noise delay errors were a few picoseconds. The delay residual (dly_{rsd}), which is mainly constructed from the atmospheric excess pass delay error, has the following proportional relationship to the Global Mapping Function Wet-term ($GMFW$),

$$\begin{aligned} dly_{rsd} &= dly_{obs} - dly_{prdc} \\ &\approx dly_{grad} \times GMFW, \end{aligned} \tag{4}$$

where $dly_{prdc} = dly_{calc} + dly_{clk} + dly_{zpdc} \times GMFW$, dly_{calc} is the predicted delay from *CALC*, and dly_{zpdc} is the correction value of the zenith pass delay. The Global Mapping Function is also used to calculate the atmospheric excess pass delay in *CALC*. The distribution of dly_{grad} arranged in accordance with azimuth is shown in Figure 7. The major distribution form of dly_{grad} appears like a sine or triangle wave. It is considered that the biggest sine wave function is made into a cause of the horizontal deviation of the station position, and the anisotropy of the atmospheric excess pass delay is mixed with the remainder after removal of the delays by the error of the station position.

However, the anisotropy of excess path delay static in time cannot by itself explain all of the delay residual variation. Even if the gradient difference is ~ 0, about 50 picoseconds of scatter is confirmed. Temporal variation of the anisotropy and other error sources that correlated with the zenith and azimuth angle are taken into consideration; for example, collaboration of the position and the structure effect of radio sources, and excess path delay error. Complexity of atmospheric structure and its timing variation also become error sources.

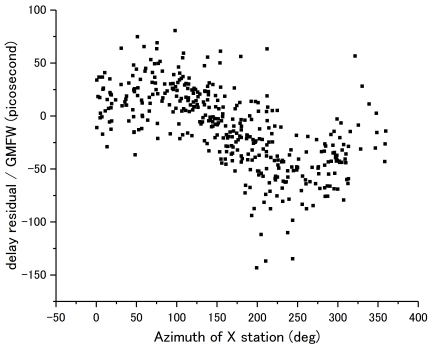

Fig. 7 The distribution of the atmospheric excess pass delay gradient in alignment with azimuth.

6 Conclusions

The wide-band fringe survey detected fringes from the VLBA Calibrator List. Detection of a fringe is recognized in a fringe with an S/N of seven or more. The detection percentage of fringes with S/N of seven or more is 80% in K- and 49% in Q-band. The minimum correlation flux density is 0.25 mJy in K-band and 0.40 mJy in Q-band. From delays of the 8-Gbps recorded VLBI data, the azimuthal anomaly residual delays, including atmospheric excess pass delay, was confirmed.

References

1. T. Jike, “VERA Geodetic VLBI with Newly Developed High-speed Sampler and Recorder”, In D. Behrend, K. Baver, and K. Armstrong, editors, IVS 2016 General Meeting Proceedings “New Horizons with VGOS”, NASA/CP-2016-219016, pages 159–162, 2016.